Desalination and Water Treatment
www.deswater.com
doi: 10.5004/dwt.2022.28625

266 (2022) 1–12
August

Energy-efficient compact multi-stage solar desalination by heat recovery with siphon mechanism for seawater feeding

Masahiro Fujiwara*, Shinobu Yamauchi

National Institute of Advanced Industrial Science and Technology (RICPT; Tohoku Center), 4-2-1 Nigatake, Miyagino-ku, Sendai, Miyagi 983-8551, Japan, emails: m-fujiwara@aist.go.jp (M. Fujiwara), yamauchi.shinobu@technopro.com (S. Yamauchi)

Received 25 January 2022; Accepted 31 May 2022

ABSTRACT

The production of freshwater from seawater using solar energy is a sustainable process for resolving water scarcity problem. For increasing the utilization efficiency of solar energy, the recycle use of the condensation heat released from water vapor is an effective method. This paper reports a solar desalination of seawater using a compact multi-stage membrane apparatus, where the membrane part for desalinating seawater by evaporation and the freshwater collecting part for reusing the condensation heat were densely piled up. In the apparatus, heat transfer and water feeding were significantly improved to increase the performance of longer time operation. A poly(methyl methacrylate) sheet with low thermal conductivity was found to be more suitable than metal sheets with high thermal conductivity for the efficient recycle of the condensation heat from water vapor. The feeding of seawater by siphon mechanism, where seawater was flowed from top to bottom, suppressed the salt deposition to maintain the performance of the freshwater production, while the desalination performance was drastically deteriorated in the multi-stage apparatuses with capillary action for seawater feeding. Using the apparatus, the energy efficiency based on the energy from irradiated sunlight reached more than 200% by the repeated recoveries of the condensation heat. Freshwater was successfully produced from actual seawater with natural sunlight.

Keywords: Seawater desalination; Solar energy; Condensation heat; Heat recovery; Siphon mechanism

1. Introduction

Seawater accounting for approximately 97.5% of water on the earth is an inexhaustible water resource. The production of freshwater from the massive amount of seawater is a potent process for solving water scarcity problem in the world [1,2]. Although various kinds of industrial plants practically produce freshwater from seawater, they are generally operated using the energy of fossil fuels. Since these processes presumably accelerate global climate change (global warming), seawater desalination by renewable energies, especially by solar energy (solar desalination), is strongly required for sustainable production of freshwater. Some review papers have summarized the recent research activities on solar desalination [3–5]. Representative solar desalination is a distillation process through the evaporation of seawater with the heat generated by solar radiation and the following condensation of water vapor [6,7]. Using a membrane distillation-based mechanism [8], we have also studied seawater desalination with sunlight [9–13]. In our latest three-ply membrane apparatus, photothermal, hydrophilic and hydrophobic membranes are piled up in the order from top to bottom. The photothermal membrane generates the heat using sunlight energy to vaporize seawater of the hydrophilic one. Water vapor permeating through the hydrophobic membrane produces desalinated freshwater by condensation [13]. Although there have been a number of examinations aimed at highly efficient solar light

* Corresponding author.

harvesting [14–19], the maximum production of freshwater is determined by solar power irradiated per unit area (which must be lower than solar constant 1,362 W/m^2) and the vaporization heat of water (more than 2,400 J/g at ambient temperature), unless the energy released by the condensation of water vapor is reused. Therefore, the recycling management of the condensation heat of water is indispensable in highly energy-efficient solar desalination.

Our latest study on solar desalination revealed that the modification of the condensation step and the effective release of the heat generated from water vapor significantly enhance the recovered volume of desalinated water [13]. It is expected that the reuse of the condensation heat for evaporating another seawater improves the energy efficiency of our desalination process fundamentally. Recently, the incorporation of the recovery of the latent heat (condensation heat) to solar desalination is highlighted for improving the usage efficiency of solar energy [20–26]. For example, a research group reported a multi-stage solar distiller with the efficiency higher than 100% by the recovery of the condensation heat [20]. They also developed sophisticated seawater distiller systems recently [25]. Another group also claimed a kind of multi-stage desalination apparatus with photovoltaic panel or sunlight absorber, where the efficiency is sufficiently higher than 100% [23]. In addition, a systematic apparatus of seawater desalination is reported with thermally localized multi-stage solar still using capillary action as seawater feeding [24]. In these processes, the part for seawater desalination and the part for condensation of water vapor are piled into multi-stages. This paper reports our latest developments of solar desalination by incorporating the recovery of the condensation heat. Our three-ply membrane apparatus was densely piled up to a multi-stage system that was designed to be totally compact for the effectual recovery of the condensation heat and its transfer to different seawater. We also improved the materials for transferring the condensation heat from usually used materials and the feeding method of seawater from capillary action.

2. Materials and methods

2.1. Materials

Polytetrafluoroethylene (PTFE) membrane used here was a PTFE membrane filter (diameter: 142 mm, thickness: 75 μm, pore size: 3.0 μm) obtained from Toyo Roshi Kaisha (ADVANTEC, Tokyo, Japan). Cellulose papers used as water wick for feeding water were filter papers purchased from Kiriyama Glass Co., Tokyo, Japan (No. 5A; diameter: 150 or 240 mm, thickness: 0.22 mm, retained particle diameter: 7 μm). These papers were cut to suitable shapes for using as water wicks. Fineshut SP ultra-black light absorbing sheet (0.2 mm thick) employed as photothermal sheet was obtained from KOYO ORIENT JAPAN CO., LTD., Saitama, Japan. Poly(methyl methacrylate) (PMMA) sheet (0.3 mm thick) was CLAREX Cast Acrylic Sheet obtained from Nitto Jushi Kogyo Co., Ltd., (Tokyo, Japan). An artificial seawater was prepared by dissolving the powder of MARINE ART SF-1 (Osaka Yakken Co., Ltd., Osaka, Japan) into a proper volume of distilled water. The contents of dissolved ions in the artificial seawater are listed in our previous paper [11]. Actual seawater was taken from Sanriku Coast of Okatsucho (Ishinomaki City, Miyagi Prefecture). After natural filtration of insoluble materials, this seawater was directly used in this study. Other materials were mainly purchased from AS ONE Corporation (Osaka, Japan).

2.2. Experiments of multi-stage apparatus with capillary action

The schematic diagram of the multi-stage apparatus where water was fed from the downside with capillary action is illustrated in Fig. 1 (taking a three-stage apparatus as an example). The apparatus was generally configured based on a Fineshut SP, water wicks made of cellulose filter papers (150 mm × 60 mm), circular PTFE membranes, spacers (silicon rubber; 1 mm thick), separators (PMMA sheet; 110 mm × 110 mm) and a Cu base plate (100 mm × 100 mm, 3.2 mm thick). Silicone rubbers as the spacer were cut to

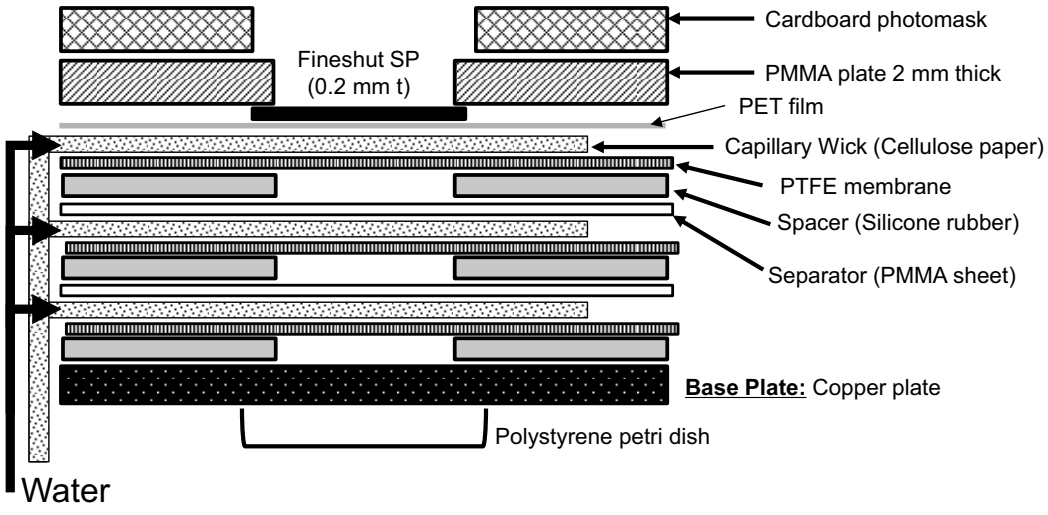

Fig. 1. Schematic diagram of the multi-stage apparatus by capillary action for water feeding (taking a three-stage system as an example).

U-shapes for opening one side of the water storage space (Fig. 2a). Condensed water was stored in the space formed by the PTFE membrane, the separator and the spacer. In general, the Cu base plate, a spacer, a PTFE membrane, a water wick and a separator were put on in the order from bottom to top. This pile was stacked in prescribed layers. A PET (polyethylene terephthalate) film (110 mm × 110 mm, 0.05 mm thick) was put on the top water wick, and a Fineshut SP (60 mm × 60 mm, 0.2 mm thick) was set on the film. The direction of water drain of the spacer was set perpendicular to the water wick (Fig. 2b). Finally, a PMMA plate (110 mm × 110 mm, 2 mm thick) with a hole (50 mm × 50 mm) at the center was put on the Fineshut. This apparatus system was firmly fastened with two wide rubber-bands and was put horizontally on a polystyrene petri dish facing upward. A cardboard photomask with 40 mm × 40 mm hole or with 60 mm × 60 mm hole was put on the top when it was used for light irradiation experiment.

In all light irradiation experiments, one end of the water wick was immersed (approximately 10 mm long) into water in a small basin. After the whole part of all wicks moistened, a simulated sunlight from a solar simulator was irradiated from directly above the apparatus to the prescribed areas of the Fineshut SP. In the case of experiments of Table 1 and Fig. 6, Solar Simulator XEF-300 (SAN-EI ELECTRIC Co., Ltd., Osaka, Japan) was employed with fixing the light irradiation range to 40 mm × 40 mm using a cardboard photomask (110 mm × 110 mm with 40 mm × 40 mm hole at the center, 3 mm thick) put on the PMMA plate. In the experiments of Tables 2 and 3 and Fig. 9, Solar Simulator XES-70S (SAN-EI ELECTRIC Co. Ltd.) was utilized with the irradiation area of 60 mm × 60 mm controlled by a cardboard photomask (110 mm × 110 mm with 60 mm × 60 mm hole at the center, 3 mm thick). The intensity of the simulated sunlight was monitored with a pyranometer (ML-01 Si-pyranometer, EKO instruments, Tokyo, Japan). The temperature of the

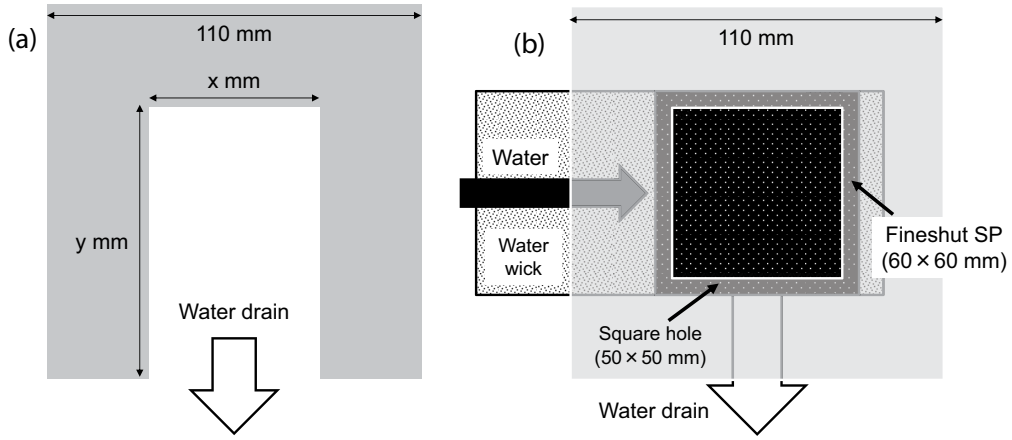

Fig. 2. (a) Shapes of spacers cut to U-shapes. x = 50, y = 80 when used in experiments of Table 1 (Irradiation area: 40 mm × 40 mm). x = 70, y = 90 when used in experiments of Tables 2 and 3 (Irradiation area: 60 mm × 60 mm). (b) Schematic diagram of the top part of the multi-stage apparatus with water feeding by capillary action.

Table 1
Volumes of recovered water with multi-stage apparatuses[a]

Run	Number of stage	Recovered water on stages (L/m²·h)				Energy efficiency (%)
		First	Second	Third	Total	
1	1	0.51	–	–	0.51	35
2	2	0.39	0.47	–	0.86	59
3	3	0.41	0.44	0.44	1.29	89
4[b]	3	0.35	0.42	0.44	1.21	83
5[c]	3	0.46	0.40	0.35	1.21	83
6[d]	3	0.32	0.29	0.23	0.84	57
7[e]	3	0.38	0.44	0.43	1.25	86
8[f]	3	0.27	0.39	0.22	0.88	60
9[f,g]	3	0.07	0.06	0.05	0.18	–

[a]Distilled water was fed with capillary action. Irradiation conditions: 1,000 W/m² for 1 h. Irradiated area: 40 mm × 40 mm using Solar Simulator XEF-300 (SAN-EI ELECTRIC Co. Ltd.). Separator: PMMA sheet (0.3 mm thick). Spacer: 1.0 mm thick. Base plate: Cu plate (3.2 mm thick). [b]Distance between PTFE membrane and separator was 0.5 mm. [c]Distance between PTFE membrane and separator was 2.0 mm. [d]PMMA plate (3 mm thick) was used as base plate. [e]Cu plate (6.4 mm thick) was used as base plate. [f]Artificial seawater (MARINE ART SF-1) was used. [g]PTFE membrane was not used.

Table 2
Seawater desalination using five-stage apparatus[a]

Time (h)	Seawater feeding method	Recovered water on stages (L/m^2)							Energy efficiency (%)
		1st	2nd	3rd	4th	5th	Drain[b]	Total	
0.5	Capillary	0.21	0.24	0.21	0.19	0.17	0.00	1.03	141
1	Capillary	0.56	0.46	0.35	0.26	0.32	0.00	1.95	133
2	Capillary	0.81	0.91	0.51	0.37	0.33	0.00	2.92	100
3	Capillary	0.39	0.50	0.64	1.12	0.46	0.00	3.10	71
4	Capillary	1.36	0.67	0.44	0.38	0.37	0.00	3.23	55
0.5	Siphon	0.31	0.27	0.25	0.19	0.16	0.00	1.19	162
1	Siphon	0.29	0.52	0.45	0.46	0.43	0.00	2.14	147
2	Siphon	0.52	0.69	0.73	0.75	0.87	0.26	3.82	131
3	Siphon	0.34	1.45	1.24	0.95	0.71	0.54	5.23	119
4	Siphon	0.77	0.83	1.04	1.40	1.91	0.00	5.95	101

[a]Artificial seawater (MARINE ART SF-1) was fed. Irradiation intensity: 1,000 W/m^2. Irradiated area: 60 mm × 60 mm using Solar Simulator XES-70S (SAN-EI ELECTRIC Co. Ltd.). [b]Volume of the recovered water collected in a rectangular vessel placed outside of the drain part of the spacer as drained water (Fig. 2).

Table 3
Seawater desalination using ten-stage apparatus[a]

Sunlight	Intensity (W/m^2)	Irradiation time (h)	Total volume of recovered water (L/m^2)	Electric conductivity (μS/cm)	Energy efficiency (%)
Simulated	1,000	1	3.16	9	216
Simulated	1,000	4	9.38	7	160
Simulated	800	4	8.29	12	177
Simulated[b]	1,000	1	4.02	–	275
Natural[c]	616[d]	4	5.59	21	152

[a]Artificial seawater (MARINE ART SF-1) was fed with siphon mechanism. Irradiated area: 60 mm × 60 mm. [b]Distilled water was fed. [c]Actual seawater was fed. [d]Average intensity of 4 h.

experimental room was controlled approximately from 18°C to 20°C by a common air conditioner. After the irradiation, water permeated through PTFE membrane was collected in the space under the PTFE membrane. Water spilled out of the space was recovered in a rectangular vessel placed outside of the drain part of the spacer as drained water (Fig. 4). The volumes of water obtained on each separator and in the drain vessel were estimated by weighing those recovered waters. Results of the water volume were the averages of several experiments, where no profound differences were found in the respective experiments. When seawater was used, the salinities of the recovered water on the first stage and the last stage (on the Cu base plate) were estimated from their electric conductivities analyzed by a conductance meter, B-771 LAQUAtwin compact conductivity meter (HORIBA, Ltd., Kyoto, Japan). Since there were not many differences between them, the electric conductivities on the first stage were listed in all tables as representatives.

2.3. Experiments of multi-stage apparatus with siphon mechanism

The experiment apparatus with siphon mechanism was based on that with capillary action, where only water wicks were changed. The schematic diagram of the experimental apparatus where water was fed from the upside with siphon mechanism (taking a three-stage system as an example) using a longer cellulose filter paper (240 mm × 60 mm) as water wick and a photo image of a ten-stage apparatus are illustrated in Figs. 3 and 4, respectively. The simulated sunlight was irradiated by Solar Simulator XES-70S (SAN-EI ELECTRIC Co. Ltd.) to the area of 60 mm × 60 mm limited by a corresponding cardboard photomask. The water level in the seawater basin (left side) was approximately 1 cm higher than the first stage of the apparatus, and the end terminal of the wick (right side) was placed at about 4 cm lower than the bottom plate. Other items and conditions were the same as those using capillary action.

2.4. Experiments of solar desalination of actual seawater with natural sunlight

The solar desalination experiment of actual seawater using natural sunlight was carried out on a roof terrace of a building in Tohoku Center of National Institute of Advanced Industrial Science and Technology (AIST Tohoku in Sendai City, Miyagi Prefecture) in a comparatively sunny day of March for 4 h (approximately 10 a.m. to 2 p.m.). In these

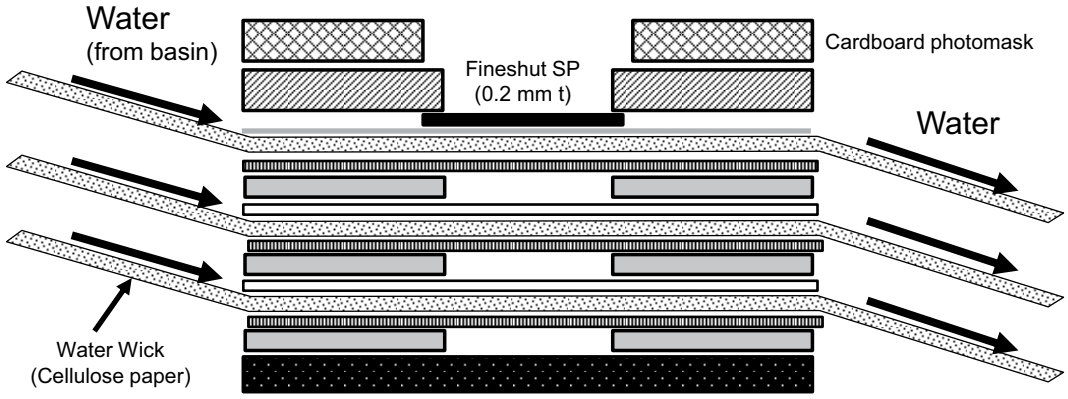

Fig. 3. Schematic diagram of the multi-stage apparatus by siphon mechanism for water feeding (taking a three-stage system as an example).

Fig. 4. An image of a ten-stage apparatus with water feeding by siphon mechanism.

experiments, the ten-stage apparatus with siphon mechanism was used. The irradiated area was limited by a cardboard photomask to 60 mm × 60 mm. The solar energy was monitored with a Solar Power Meter SPM-SD (SATO TECH, Kanagawa, Japan) at the same time. Other experimental procedures were similar to those with simulated sunlight.

2.5. Estimation of energy efficiency

The energy efficiency was calculated by the recovered volumes of water and the energy of the irradiated light using the following equation [13]:

$$\eta(\%) = \frac{H_v}{Q_e} \times 100 \quad (1)$$

where η is energy efficiency, H_v is the vaporization heat of the recovered volumes of water, and Q_e is the energy of the irradiated sunlight to the prescribed areas. The vaporization heat at 20°C was employed in this calculation, because the initial temperature of water or seawater was approximately 20°C in most experiments. Since the energies used for the vaporization of unrecovered water and for heating water with temperature elevation were excluded in this calculation, the energy efficiencies presented in this paper are regarded as the minimum values of the efficiency.

2.6. Temperature measurements

The temperature variations of hot water on PMMA sheet or Al sheet were monitored by the following way. To a thermocouple attached on the top surface of PMMA or Al sheet, 1 mL of hot water (approximately 90°C) was dropped. The measurement of the temperature was started just before the dropping. The temperature variations of the back side of PMMA sheet or Al sheet were monitored by the analogous manner, where the thermocouple was attached on the bottom surface of PMMA or Al sheet. Thermography images were recorded by an infrared thermography camera Testo 871 (Testo K.K., Kanagawa, Japan). The temperature of the experimental room was controlled at around 22°C by a common air conditioner. The images of Fineshut SP were taken from obliquely upward under the irradiation

of simulated sunlight from directly above (1,000 W/m^2). The images showing thermal conductions in PMMA or Al sheets from hot water were monitored from directly above after dropping 1 mL of hot water.

2.7. Scanning electron microscope observation

Scanning electron microscope (SEM) images of water wicks were obtained by JEOL JSM-6390 electron microscope (Tokyo, Japan) after using for the desalination with five-stage apparatus under the irradiation of simulated sunlight at the intensity of 1,000 W/m^2 for 2 h.

3. Results and discussion

3.1. Performances of multi-stage apparatuses with capillary action

At first, the effect of the stage number of multi-stage apparatus on the performance of water treatment is examined. Capillary action from the downside is employed as water feeding with a water wick of cellulose filter paper. In the optimizing stage of our multi-stage apparatus, distilled water was employed, because of the high reproducibility and the efficiency of those experiments. A black light absorbing sheet (Fineshut SP) is utilized as a photothermal sheet as is the case with our latest paper [13], which generated heat by light irradiation. Fig. 5 illustrates thermography images of the light absorbing sheet under the irradiation of simulated sunlight at the intensity of 1,000 W/m^2. The temperature of the central part of the sheet rapidly increased with irradiation time. After 30 s irradiation, the temperature reached 31.8°C from 22°C. Since the elevation of the temperature from 3 to 5 min irradiation was slight (from 35.6°C to 36.0°C), it is likely that the generation and release of heat came to equilibrium after 5 min irradiation. The temperature decreased to 25°C at 1 min after stopping 5 min irradiation.

The schematic diagram of the multi-stage apparatus is shown in Fig. 1. In a single stage apparatus for the water

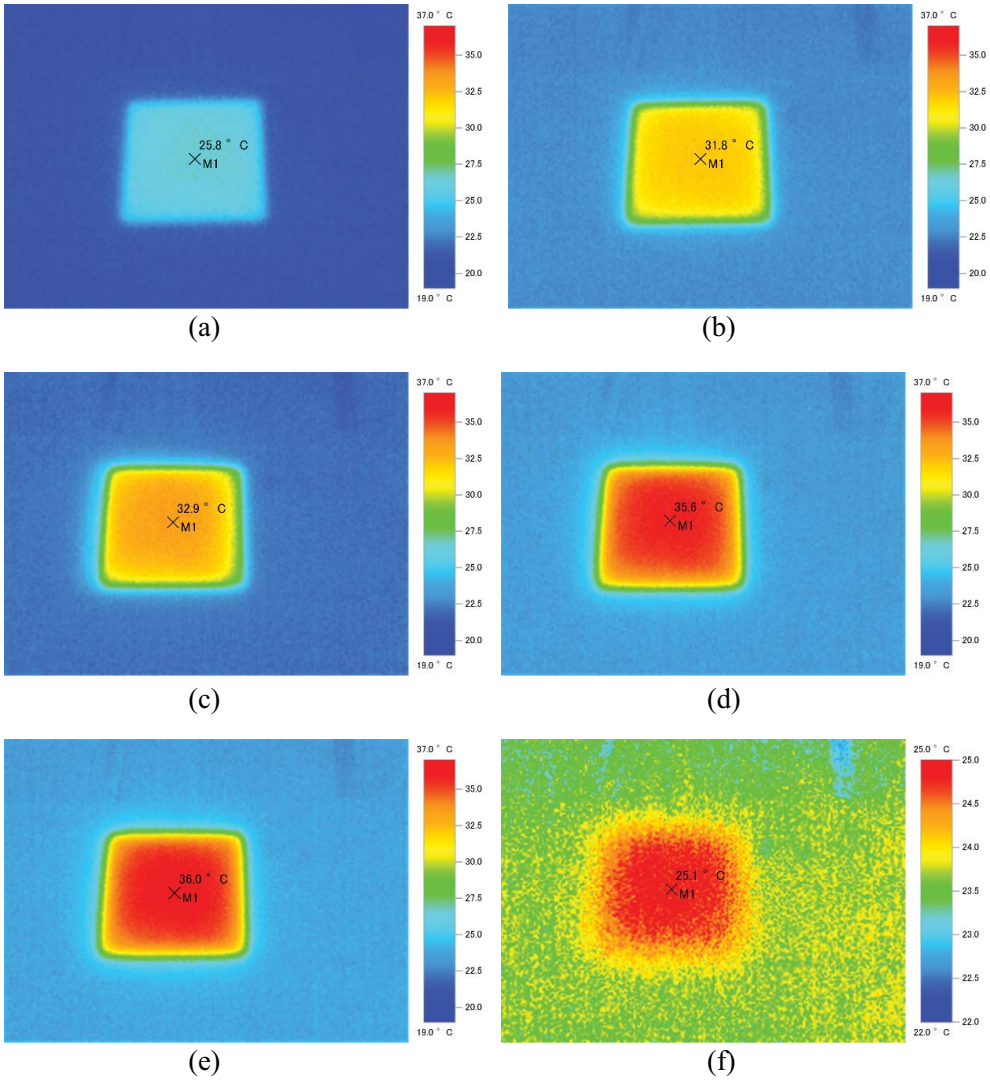

Fig. 5. Thermography images of a light absorbing sheet (Fineshut SP) under the irradiation of simulated sunlight (1,000 W/m^2). (a) 5 s irradiation, (b) 30 s irradiation, (c) 1 min irradiation, (d) 3 min irradiation, (e) 5 min irradiation, and (f) 1 min after stopping irradiation.

treatment experiment, the water wick was sandwiched between the light absorbing sheet and PTFE membrane. A silicone rubber spacer with empty space for storing permeated water (Fig. 2a) and a Cu base plate were set under the PTFE membrane. In multi-stage apparatuses, separator sheets and different water wicks were incorporated under the silicone rubber spacers. As listed in Table 1 using distilled water, 0.51 L/m²·h of water was collected under the PTFE membrane in the single stage apparatus (run 1). In the cases of multi-stage apparatuses using PMMA sheet as the separator, the permeated water through the PTFE membrane was found even on the second and third stages (runs 2 and 3). The recovered volumes of the waters on these stages were slightly higher than that on the first stage, and the total volume of the recovered waters increased with the number of the stages. It is clear that the condensation heat generated from water vapor was successfully reused to evaporate water in the water wick just beneath. The energy efficiency of the three-stage apparatus reached nearly 90%, while the efficiency of our latest study using heatsinks was around 60% [13]. The distance of 1 mm between the PTFE membrane and the separator was optimal. The experiments with the distance of 0.5 or 2.0 mm controlled by the thickness of the silicon rubber spacer showed slightly lower volumes of recovered water (runs 4 and 5). The material of the base plate was also an important factor. When a PMMA plate (3 mm thick) was used instead of the Cu plate (3.2 mm thick), the total volume of the water was considerably reduced from 1.29 to 0.84 L/m²·h (run 6). While the temperature of Cu plate (3.2 mm thick) was increased more than 5°C after the experiment, the temperature elevation of the PMMA plate was less than 2°C. The Cu plate with high heat conductivity (the heat conductivity of Cu at 300 K: 402 W/m·K [27]) efficiently released heat to promote the condensation of water vapor. On the other hand, the limited release of heat by the low heat conductivity of the PMMA plate (the heat conductivity at 300 K: 0.15 W/m·K [27]) hindered the condensation. A thicker Cu plate (6.4 mm thick) had no clear enhancing effect on the volume of water (run 7). Thus, the distance between the PTFE membrane and the separator was fixed to 1 mm, and the Cu plate (3.2 mm thick) was employed as base plate in the following experiments.

3.2. Effect of materials of the separator

The material of the separator placed between silicone rubber spacer and water wick was a crucial factor for the performance of the apparatuses. In the recycle use of the condensation heat, the heat must be efficiently transported to another water wick for vaporizing different water. In the researches directed for the recovery of the condensation (latent) heat [20,21,23–26], the metallic separators with high heat conductivity, mainly Al metal materials (the heat conductivity of Al at 300 K: 237 W/m·K [27]), were exclusively used. Fig. 6 summarized the effect of the separator sheet on the volume of recovered water in the three-stage apparatus. When metallic Al (0.1 mm thick) and Cu sheets (0.4 mm thick) were employed as the separator, the volumes of the recovered water were significantly reduced compared with the case with PMMA sheet. Another plastic polymer sheet PVC (polyvinyl chloride; the heat conductivity at 300 K: 0.16 W/m·K [27]) showed an analogous result to the PMMA sheet. Thus, these polymer sheets with low heat conductivity were more effective than Al and Cu sheets in our apparatus. The temperature variations of water on the PMMA sheet and the Al sheet were compared using 1 mL of hot distilled water (about 90°C) as illustrated in Fig. 7a. The temperature of the water on the PMMA sheet decreased more slowly than that on the Al sheet. After 2 min, the temperature difference reached approximately 5°C.

The temperature variations of the back sides right below the hot water revealed the transfer of the condensation heat more directly. As illustrated in Fig. 7b, in the case of the Al sheet, after the rapid elevation to about 60°C, the temperature instantly decreased. Within 4 min, the temperature of the sheet returned to the original one. On the other hand, the temperature increase of the PMMA sheet was slow and the temperature gradually decreased. Approximately 10 min was required to return to the original temperature. Fig. 8 illustrates the thermography images of 1 mL of hot water on PMMA sheet or on Al sheet at 120 s after the hot water was dropped. In the image of the PMMA sheet (Fig. 8a), although the domain of the water was observed as light blue domain, no region of the PMMA sheet was detected. On the other hand, in the image of Al sheet (Fig. 8b), square Al sheet was dimly observed with a pale domain of cooled water. This image indicated that the heat of the hot water was transferred to all part of the Al sheet within 120 s, while the heat of the hot water scarcely spread into the PMMA sheet. These observations are well consistent with the results of the temperature observation shown in Fig. 7 that the PMMA sheet conserved the heat from the hot water longer than the Al one. It is thought that the longer retention of the heat in the PMMA sheet achieved the efficient reuse of the condensation heat, resulting in the recovery of higher volumes of water. Little

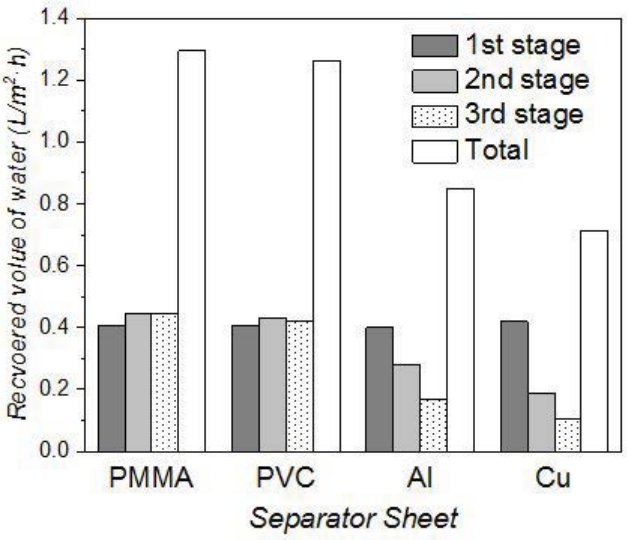

Fig. 6. Effect of the separator sheets on the volume of the recovered water on each stage. Distilled water was fed with capillary action. Irradiation conditions: 1,000 W/m² for 1 h. Irradiated area: 40 mm × 40 mm. Spacer: 1.0 mm thick. Base plate: Cu plate (3.2 mm thick).

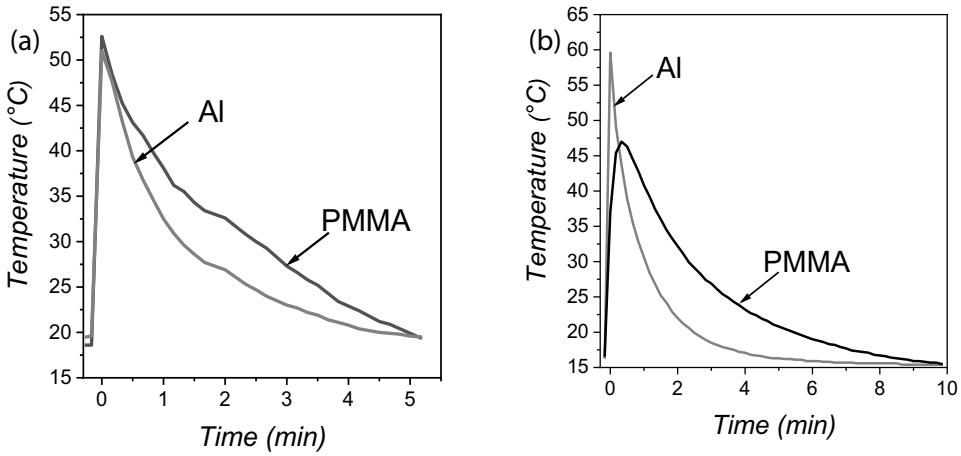

Fig. 7. (a) Temperature variations of hot water (approximately 90°C) on PMMA sheet or Al sheet. (b) Temperature variations of the back side of PMMA sheet or Al sheet directly below the hot water. Temperatures were monitored using thermocouples.

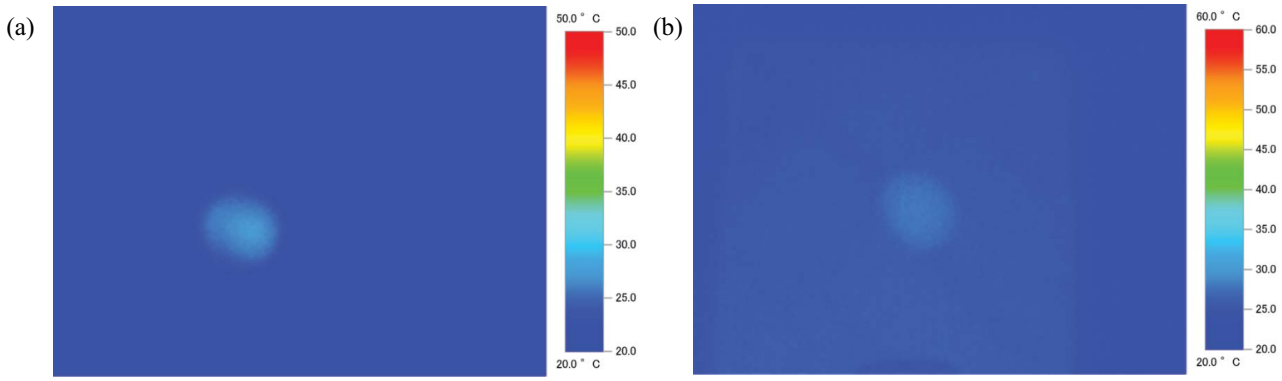

Fig. 8. Thermography images of hot water on PMMA sheet (a) and on Al sheet (b) after 120 s of its dropping.

difference among the collected volumes of the water on the first, second and third stages (Fig. 6) indicated the transport of the condensation heat to the third stage with low heat loss in the cases using the PMMA and PVC sheet. The heat was finally released with the Cu plate that was placed at the bottom of the apparatus. These findings suggested that further increases of the stage number are possible when those polymer sheets are used. On the other hand, when the Al and Cu sheets were employed, the collected volumes of the water clearly decreased with the stage number. The volume on the first stage, which was directly formed by the photothermal effect of the light absorbing sheet, accounted for roughly half of the total volume of the recovered water. It is obvious that the transfer of the condensation heat at the first stage to the second and third stages was insufficient. In these metal sheets, the heat readily spreads to the whole area to reduce the reuse efficiency of the heat for the vaporization of water. The increase of the stage number of the apparatuses with these metal sheets will be useless for enhancing the volume of the recovered water.

3.3. Effect of the utilization of PTFE membrane

The mechanism of our apparatus is based on membrane distillation [8,28–30], which utilizes the properties of hydrophobic membrane that the penetration of liquid water is prevented, and that the permeation of gaseous water vapor is permitted. Since water soaked up with capillary action does not naturally drop from the water wick, it seems that the hydrophobic PTFE membrane is not essential even in our apparatus [24]. Then, the same experiments were compared with or without the PTFE membrane, where artificial seawater (MARINE ART SF-1) was used instead of distilled water. The results are also listed in Table 1. With the PTFE membrane, 0.88 L/m^2·h of water was recovered totally (run 8). The electric conductivity of the water was less than 100 μS/cm (salinity less than 0.01%) to show that the multistage apparatus was active for seawater desalination. On the other hand, when the PTFE membrane was not used (run 9), the volume of the recovered water was decreased to 0.18 L/m^2·h, whose electric conductivity reached to 6.4 × 10^3 μS/cm. As the electric conductivity of the original artificial seawater was about 20 × 10^3 μS/cm, the recovered water was scarcely desalinated. It is thought that the drops of the condensed water on the separator contacted the water wick to be mixed with seawater. Therefore, the electric conductivity of the water was comparable with the original seawater. The decrease of the volume of the collected water is due to the absorption of the condensed water to the wick. In the case using PTFE membrane, even when the drop of the condensed

water contacted the membrane, no seawater in the wick contaminated the water by the barrier of the PTFE membrane. Although the contamination of seawater might be avoidable by extending the distance between the water wick and the separator even in the apparatus without the membrane, the results in Table 1 revealed that the wider distance between them decreased the volume of the recovered water (run 5).

For fabricating compact seawater desalination apparatus, the PTFE membrane separating seawater and desalinated freshwater is an indispensable item. From these results, the components of the compact multi-stage apparatus were established as follows. The most suitable distance between the PTFE membrane and the separator was 1.0 mm. The PMMA sheet (0.3 mm thick) was the most efficient separator. The Cu plate (3.2 mm thick) is effectual as the bottom plate. The PTFE membrane was essential for downsizing the desalination apparatus. Fig. 9 illustrates the dependence of the total volume of the recovered water on the number of all stages of the apparatus thus optimized by the above-described examinations. The irradiated area of simulated sunlight was increased to 60 mm × 60 mm, which area was basically employed in the following seawater desalination experiments. The proportional increase of the total volume of the recovered water was observed in the apparatuses with from one to three stages, indicating the effective recycling of the condensation heat in all stages. Although the increase rate of the water volume was slowed down in the apparatuses with more than five stages, the total recovered volume of the apparatus with ten stages was significantly higher than that with three stages. Thus, the condensation heat was recyclable to the tenth stage.

3.4. Solar desalination of seawater with capillary action

Using the apparatus established by the experiments above, seawater desalination using solar energy was examined by feeding the artificial seawater with capillary action. In these experiments, a wider irradiation area (60 mm × 60 mm) was employed for producing more volume of freshwater using another Solar Simulator (XES-70S; SAN-EI ELECTRIC Co. Ltd.). The number of the stages was also increased to five in these experiments. Results are summarized in Table 2. As is the case of single stage apparatuses [10–13], the water volumes recovered under PTFE membrane from artificial seawater became lower than those from distilled water in the case of the multi-stage apparatuses. The electric conductivities of all experiments listed in Table 2 were lower than 30 μS/cm to indicate that the salinities of the collected water were estimated to be less than 0.01%. Therefore, the artificial seawater was successfully desalinated to freshwater. After the irradiation for 0.5 h, about 1.03 L/m^2 of water was recovered in the five stages totally with 0.17 L/m^2 of water on the fifth stage. Little difference among the volumes recovered on each stage indicated that the condensation heat was efficiently recycled in all stages to produce freshwater more than simply estimated from the provided light energy, because the energy efficiency estimated from the total volume of the recovered water exceeded 100% (141%).

While the recovered freshwater roughly doubled from 0.5 to 1 h, the volume was scarcely increased by the irradiation longer than 2 h. Fig. 10 illustrating the time course of the total volumes of the recovered freshwater clearly shows this plateaued trend. In the apparatuses using capillary action for seawater feeding, seawater is supplied from a lower terminal of a water wick to a higher terminal that is exposed to the irradiated light. The concentration of seawater at the light irradiated area gradually increased with time to induce the depression of water vapor pressure. Finally, the precipitation of salts from seawater occurred in the wick, which constrained the flux of water vapor to the PTFE membrane. Fig. 10 also indicates the time course

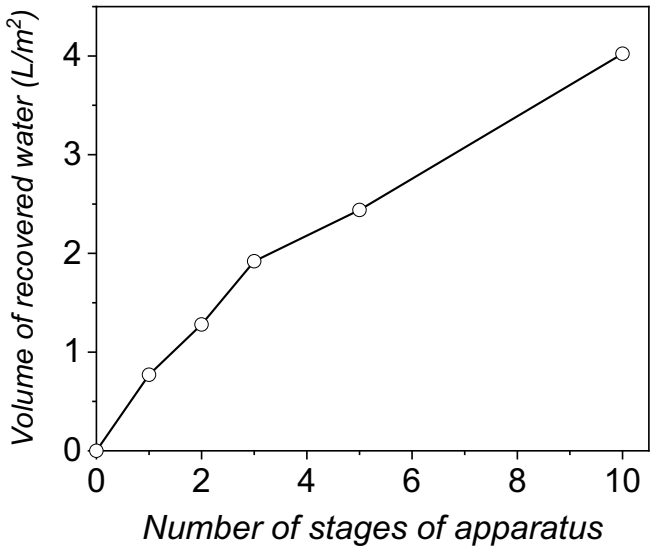

Fig. 9. Total volumes of the recovered water as a function of the number of all stages of apparatuses. Distilled water was fed with capillary action. Irradiation conditions: 1,000 W/m^2 for 1 h. Irradiated area: 60 mm × 60 mm.

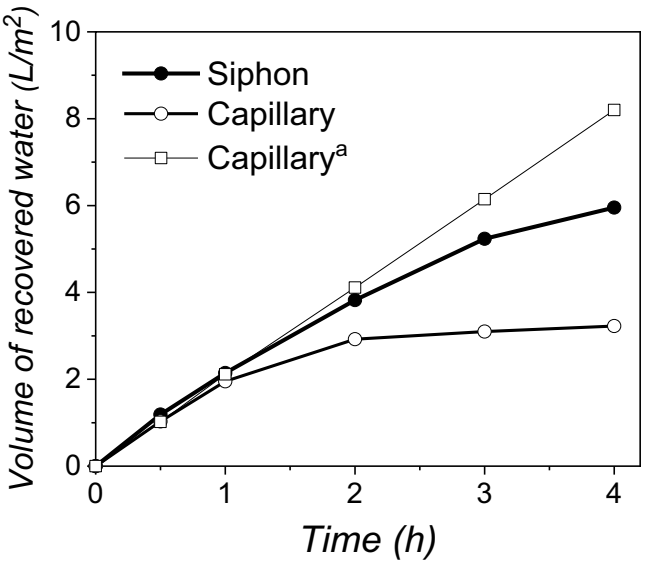

Fig. 10. Time courses of the total volumes of the recovered water using five-stage apparatus with artificial seawater. [a]With distilled water.

of the total volumes of the recovered water, when distilled water was fed with capillary action. The recovered volume of water increased proportionally with time in contrast to the case using seawater. The application of distilled water naturally led neither to the increase of seawater concentration nor to the deposition of salts. Therefore, it is obvious that the degradation of the performance of solar desalination is attributed to the utilization of seawater. Since the concentrated seawater and the deposited salts in the water wick cannot be eliminated during desalination process, appropriate treatments are required for cleaning up the wick after the completion of the desalination process. For example, the reverse flow of fresh seawater [20] or keeping the water wick soaked in fresh seawater without light irradiation for long time [24] are carried out for washing the wicks. Thus, when seawater is supplied by capillary action, the deterioration of the desalination performance is an unavoidable issue in long-time operation.

3.5. Solar desalination of seawater with siphon mechanism

Next, we used a siphon mechanism instead of capillary action for feeding seawater. In this process, seawater was supplied with the water wick from a basin placed higher level to another end terminal through the region exposed to the irradiated light. The schematic diagram and the image of the multi-stage apparatus with siphon mechanism are illustrated in Figs. 3 and 4, respectively. A major difference from the apparatus with capillary action is that the end terminal of the wick is placed outside of the irradiation region for discharging concentrated seawater, which is unrealizable by capillary action. The results of the desalination by this siphon mechanism apparatus are also listed in Table 2. The collected waters were desalinated to freshwater in the cases of siphon mechanism as well. Within 1 h irradiation, the volumes of freshwater obtained were approximately the same as those of the experiments with capillary action. On the other hand, 5.95 L/m^2 of freshwater was recovered by 4 h irradiation, which was significantly higher than that with capillary action (3.23 L/m^2). As illustrated in Fig. 10, the recovered volume of freshwater basically increased with irradiation time in contrast to the case of the capillary action. However, as compared with the recovered volume using distilled water, the moderate depression effect was observed even in the case of siphon mechanism. SEM images shown in Fig. 11 illustrate the water wicks used in the desalination experiments for 2 h with capillary action or with siphon mechanism, respectively. From the images of the used wick with capillary action (Fig. 11a), a number of large and small crystals were found. On the other hand, the strings of cellulose looked nearly clean according to the images of the wick used in the apparatus with siphon mechanism (Fig. 11b). Different from the case with capillary action, the siphon mechanism considerably restricted the formation of concentrated seawater and the deposition of salts by the continuous flow of seawater to the end terminal of the water wick during the desalination treatment.

At the initial stage up to 1 h irradiation, the volume of the recovered water with capillary action was nearly equal to that with siphon mechanism and that using distilled water. These observations indicated that the basic performance of the apparatus with capillary action is similar to that with siphon mechanism. As mentioned in introduction part, our solar desalination consists of the following three steps, the generation of heat with irradiated light energy, the evaporation of seawater with the heat and the condensation of water vapor. The proper operation of all these three steps is necessary for efficient solar desalination. However, in the case using capillary action, the step of the evaporation of seawater was obstructed by the increase of seawater concentration and the deposition of salts to deteriorate the whole performance of the apparatus. The apparatus with siphon mechanism significantly suppressed the increase and the deposition by flowing seawater through the wick, achieving the better production of freshwater even after 4 h. Although the advantage of the siphon mechanism was thus ascertained, the apparatus with the siphon mechanism must be designed with consideration of hydraulic head especially in the case of increasing in size.

3.6. Solar desalination of seawater using ten-stage apparatus with siphon mechanism

Seawater desalination was attempted using a ten-stage apparatus with the siphon mechanism. The results of these experiments are summarized in Table 3. This apparatus was compact in size even when ten stages were piled up. The thickness of the ten-stage apparatus was approximately 22 mm due to the short distance (1 mm) between the PTFE membrane and the PMMA separator (Fig. 4). When

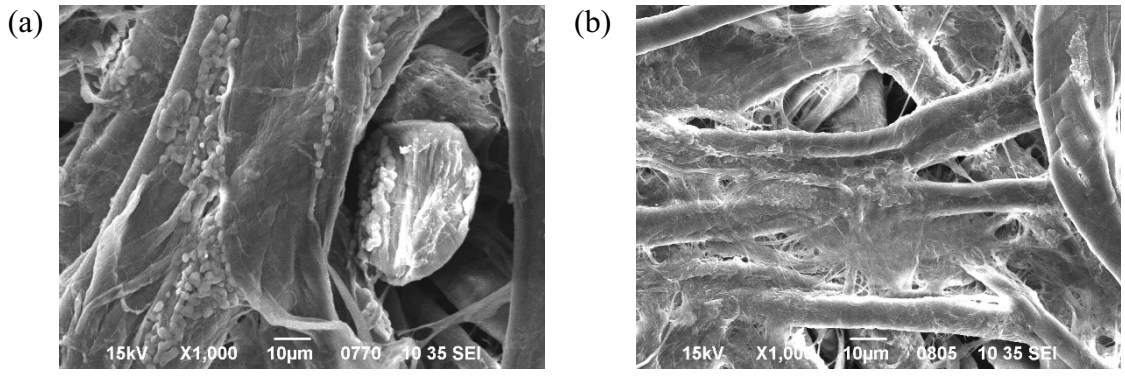

Fig. 11. SEM images of a water wick used for desalination with capillary action (a) and with siphon mechanism (b).

simulated sunlight at the intensity of 1,000 W/m^2 was irradiated for 1 h, 3.16 L/m^2·h of water was obtained from the artificial seawater on ten-stages in total. Even on the tenth stage, 0.21 L/m^2·h of water was recovered to show that the heat recycle was reached to the tenth stage. The recovered volumes (L/m^2·h) of water on each stage are as follows; 1st: 0.54, 2nd: 0.43, 3rd: 0.38, 4th: 0.33, 5th: 0.28, 6th: 0.28, 7th: 0.28, 8th: 0.28, 9th: 0.19 and 10th: 0.21. Since the electric conductivity of the recovered water was less than 10 μS/cm, the recovered water was evaluated to be desalinated freshwater. The energy efficiency reached more than 200% (216%). When distilled water was used, the efficiency reached 275%. After 4 h irradiation, 9.38 L/m^2 of freshwater was obtained, where the average productivity of freshwater was calculated to approximately 2.35 L/m^2·h and 2.35 L/kWh with a high energy efficiency (160%). Even when a weaker sunlight at the intensity of 800 W/m^2 was used, a large volume of freshwater (8.29 L/m^2) was obtained by 4 h irradiation with a high energy efficiency of 177%.

Finally, the desalination of actual seawater with natural sunlight was examined with the ten-stage apparatus. The apparatus was placed on an outdoor place in our institute (AIST Tohoku in Sendai City) for about 4 h in March (nearly from 10 a.m. to 2 p.m.). The result is also listed in Table 3, and the monitored intensity of sunlight insolation is illustrated in Fig. 12. About 5.6 L/m^2 of desalinated water was produced from actual seawater by natural sunlight irradiated to the area of 3.6×10^{-3} m^2 (60 mm × 60 mm) for 4 h. The recovered water was sufficiently desalinated according to their electric conductivities, and the energy efficiencies were beyond 100%. The average productivity of freshwater was estimated to approximately 1.40 L/m^2·h and 2.27 L/kWh. According to a report [31], 1.5 L of drinking water is required for one person per one day. Therefore, the irradiation area of about 0.27 m^2 for 4 h is sufficient for producing the drinkable freshwater even using the mild sunlight of March. When a strong sunlight in summer (at the intensity of 1,000 W/m^2) is available, the sunlight irradiation to 0.16 m^2 for 4 h is enough to produce the volume of freshwater. Thus, our solar desalination apparatus was considerably developed toward practical use. For the application of our apparatus to actual process, longer-time tests under various weather conditions are essential. In addition, further optimizations of the apparatus are necessary for enhancing the performance of the freshwater production, especially for overcoming the performance degradation in long-time operation.

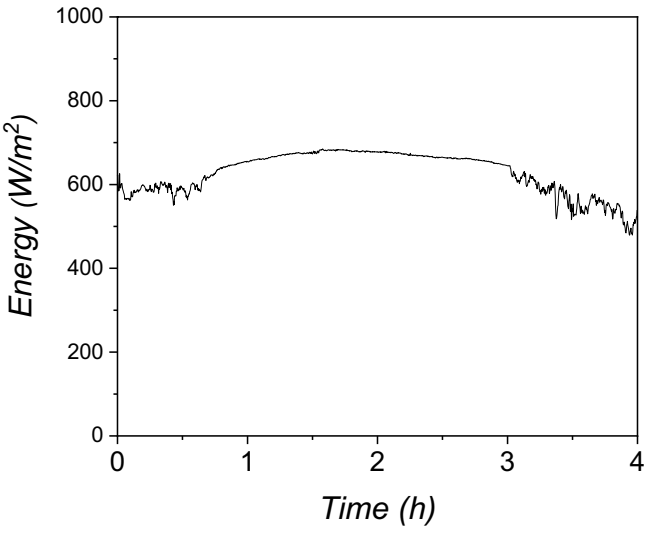

Fig. 12. Intensity of natural sunlight in the experiment "Natural" of Table 3.

3.7. Consideration on the improvement of solar desalination of seawater in our multi-stage apparatus

This paper reveals some features of our improved multi-stage apparatus for solar desalination of seawater. The compact multi-stage apparatus was assembled using PTFE membrane, which enabled densely piled-up stages with the distance between each stage of 1 mm and the whole thickness of the ten-stage apparatus of approximately 22 mm. Since the main purpose of the multi-stage apparatuses is the recycling of the condensation heat from water vapor, highly heat-conductive material sheets have been considered to be effective for the efficient transfer of the condensation heat and exclusively employed as the separator [20–26]. On the other hand, this paper concluded from our optimized apparatus that plastic material sheets like PMMA one with low thermal conductivity are more suitable than the highly heat-conductive material ones. The condensation heat spreads quickly throughout the highly heat-conductive material sheets to result in the loss of the heat. It is likely that the high performances of reported apparatuses are attributed to that the multi-stage apparatuses are introduced into heat retaining containers for reducing the overall heat loss. When low heat-conductive material sheets were used as separator, the condensation heat retained in the sheets for a long time secured the efficient transfer of the heat to another seawater wick even when the apparatus was not put in the heat retaining container. On the other hand, as shown in Fig. 9, the decrease of the heat transfer efficiency with the total number of the stages indicated that the heat release occurred even in our apparatus. For enhancing the energy efficiency of our apparatus, some heat insulation mechanism should be incorporated.

In general, the distillation method of seawater desalination is scarcely affected by the concentration of seawater in contrast to reverse osmosis method [2]. However, the performance degradation of desalination caused from the increased seawater concentration and the resulting salt deposition in the domain of seawater feeding wicks exposed to sunlight is an unavoidable problem of multi-stage apparatuses using capillary action. Therefore, some cleaning up processes of the wicks are essentially required [20,24]. On the other hand, the siphon mechanism reported in this paper for seawater feeding is a water flow system, where seawater is not remained in the sunlight-irradiated region to restrict the degradation of the desalination performance. Since the decrease of the freshwater production was observed even with the siphon mechanism (Fig. 10), the balanced feeding rate of seawater with the freshwater production by the permeation of water vapor through PTFE membrane will be required.

4. Conclusion

This paper reports a compact multi-stage apparatus of solar desalination of seawater, where the mechanism of recycling the condensation heat of water vapor is installed. The energy efficiency based on the recovered volume of water and the energy of irradiated sunlight reached more than 200% by the repeated reuse of the condensation heat with ten-stage apparatus. Various parts of our apparatus were substantially modified for creating a compact energy-efficient multi-stage apparatus for solar desalination. The employment of hydrophobic PTFE membranes between each stage achieved the densely piled-up compact apparatus. Especially, the heat transfer and water feeding of the apparatus were significantly improved to increase the desalination performance especially for long timer operation. A PMMA sheet with low thermal conductivity was effective for the recycle of the condensation heat from water vapor, while metal sheets with high thermal conductivity were insufficient. While the degradation of the performance of solar desalination inevitably occurred by increasing the concentration of seawater and by the resulting salt deposition when seawater is fed by capillary action, they are improved by the flow feeding of seawater from the upside with siphon mechanism to achieve the longer time operation. Freshwater was successfully produced from actual seawater with the energy efficiency of more than 100%, even when natural sunlight was used in the ten-stage apparatus.

Acknowledgement

This work was supported by a Grant-in-Aid for Scientific Research (Grant Number: JP19H04331) from the Japan Society for the Promotion of Science (JSPS). Authors appreciate Dr. Mitsuhiro Kanakubo (National Institute of Advanced Industrial Science and Technology; AIST) and Dr. Satoshi Ishii (National Institute for Materials Science; NIMS) for their helps and discussion to this study.

References

[1] M. Elimelech, W.A. Phillip, The future of seawater desalination: energy, technology, and the environment, Science, 333 (2011) 712–717.
[2] T. Tong, M. Elimelech, The global rise of zero liquid discharge for wastewater management: drivers, technologies, and future directions, Environ. Sci. Technol., 50 (2016) 6846–6855.
[3] C. Li, Y. Goswami, E. Stefanakos, Solar assisted seawater desalination: a review, Renewable Sustainable Energy Rev., 19 (2013) 136–163.
[4] H. Sharon, K.S. Reddy, A review of solar energy driven desalination technologies, Renewable Sustainable Energy Rev., 41 (2015) 1080–1118.
[5] X. Yu, Q. Zhang, X. Liu, N. Xu, L. Zhou, Salt-resistive photothermal materials and microstructures for interfacial solar desalination, Front. Energy Res., 9 (2021) 721407, doi: 10.3389/fenrg.2021.721407.
[6] A.E. Kabeel, S.A. El-Agouz, Review of researches and developments on solar stills, Desalination, 276 (2011) 1–12.
[7] A. Kaushal, Varun, Solar stills: a review, Renewable Sustainable Energy Rev., 11 (2010) 446–453.
[8] M. Suleman, M. Asif, S.A. Jamal, Temperature and concentration polarization in membrane distillation: a technical review, Desal. Water Treat., 229 (2021) 52–68.
[9] M. Fujiwara, T. Imura, Photo induced membrane separation for water purification and desalination using azobenzene modified anodized alumina membranes, ACS Nano, 9 (2015) 5705–5712.
[10] M. Fujiwara, Water desalination using visible light by disperse red 1 modified PTFE membrane, Desalination, 404 (2017) 79–86.
[11] M. Fujiwara, M. Kikuchi, Solar desalination of seawater using double-dye-modified PTFE membrane, Water Res., 127 (2017) 96–103.
[12] M. Fujiwara, M. Kikuchi, K. Tomita, Freshwater production by solar desalination of seawater using two-ply dye modified membrane system, Desal. Water Treat., 190 (2020) 1–11.
[13] M. Fujiwara, K. Takahashi, K. Takagi, Improvement of condensation step of water vapor in solar desalination of seawater and the development of three-ply membrane system, Desalination, 508 (2021) 115051, doi: 10.1016/j.desal.2021.115051.
[14] S. Ben Abdallah, N. Frikha, S. Gabsi, Study of the performances of different configurations of seawater desalination with a solar membrane distillation, Desal. Water Treat., 52 (2014) 2362–2371.
[15] Z. Mao, Y. Chen, J. Ren, C. Guo, H. Liu, J. Gao, Development of a miniature low-temperature solar seawater desalination device, Desal. Water Treat., 170 (2019) 24–37.
[16] Q. Fan, L. Wu, Y. Liang, Z. Xu, Y. Li, J. Wang, P.D. Lund, M. Zeng, W. Wang, The role of micro-nano pores in interfacial solar evaporation systems – a review, Appl. Energy, 292 (2021) 116871, doi: 10.1016/j.apenergy.2021.116871.
[17] F. Meng, B. Ju, S. Zhang, B. Tang, Nano/microstructured materials for solar-driven interfacial evaporators towards water purification, J. Mater. Chem. A, 9 (2021) 13746–13769.
[18] J.-T. Wang, J.-L. Hong, Effect of folding on 3D photothermal cones with efficient solar-driven water evaporation, Appl. Therm. Eng., 178 (2020) 115636, doi: 10.1016/j.applthermaleng.2020.115636.
[19] A. Khalil, F.E. Ahmed, N. Hilal, The emerging role of 3D printing in water desalination, Sci. Total Environ., 790 (2021) 148238, doi: 10.1016/j.scitotenv.2021.148238.
[20] E. Chiavazzo, M. Morciano, F. Viglino, M. Fasano, P. Asinari, Passive solar high-yield seawater desalination by modular and low-cost distillation, Nat. Sustainability, 1 (2018) 763–772.
[21] D. Ghim, X. Wu, M. Suazo. Y.-S. Jun, Achieving maximum recovery of latent heat in photothermally driven multi-layer stacked membrane distillation, Nano Energy, 80 (2021) 105444, doi: 10.1016/j.nanoen.2020.105444.
[22] X. Mu, Y. Gu, P. Wang, A. Wei, Y. Tian, J. Zhou, Y. Chen, J. Zhang, Z. Sun, J. Liu, L. Sun, S. Tanemura, L. Miao, Strategies for breaking theoretical evaporation limitation in direct solar steam generation, Sol. Energy Mater. Sol. Cells, 220 (2021) 110842, doi: 10.1016/j.solmat.2020.110842.
[23] W. Wang, Y. Shi, C. Zhang, S. Hong, L. Shi, J. Chang, R. Li, Y. Jin, C. Ong, S. Zhuo, P. Wang, Simultaneous production of freshwater and electricity via multistage solar photovoltaic membrane distillation, Nat. Commun., 10 (2019) 3012, doi: 10.1038/s41467-019-10817-6.
[24] Z. Xu, L, Zhang, L. Zhao, B. Li, B. Bhatia, C. Wang, K.L. Wilke, Y. Song, O. Labban, J.H. Lienhard, R. Wang, E.N. Wang, Ultrahigh-efficiency desalination *via* a thermally-localized multistage solar still, Energy Environ. Sci., 13 (2020) 830–839.
[25] M. Morciano, M. Fasano, L. Bergamasco, A. Albiero, M.L. Curzio, P. Asinari, E. Chiavazzo, Sustainable freshwater production using passive membrane distillation and waste heat recovery from portable generator sets, Appl. Energy, 258 (2020) 114086, doi: 10.1016/j.apenergy.2019.114086.
[26] W. Wang, S. Aleid, Y. Shi, C. Zhang, R. Li, M. Wu, S. Zhuo, P. Wang, Integrated solar-driven PV cooling and seawater desalination with zero liquid discharge, Joule, 5 (2021) 1873–1887.
[27] Handbook of Chemistry: Pure Chemistry, 4th ed., Pt. 2, The Chemical Society of Japan (Eds.), Marzen, Tokyo, 1993, pp. 66–70 (in Japanese).
[28] A. Alkhudhiri, N. Darwish, N. Hilal, Membrane distillation: a comprehensive review, Desalination, 287 (2012) 2–18.
[29] M. Khayet, Solar desalination by membrane distillation: dispersion in energy consumption analysis and water production costs (a review), Desalination, 308 (2013) 89–101.
[30] K.W. Lawson, D.R. Lloyd, Membrane distillation, J. Membr. Sci., 124 (1997) 1–25.
[31] E. Jéquier, F. Constant, Water as an essential nutrient: the physiological basis of hydration, Eur. J. Clin. Nutr., 64 (2010) 115–123.